

Thrust Generation Through a Collimated Electron Beam in a Magnetic Mirror and its Possible Applications in Plasma Thrusters

Luis A. Fernández-Ramos, José E. Mendoza-Torres



Abstract: In this article, we apply some basic concepts of electric thrusters, using Monte Carlo simulations. One such concept is the thrust, which we calculate for the simulated case of a simple thruster, consisting of two stages. The goal is to study the thrust in a magnetic bottle as a function of the collimation of an assembly of particles. In the first stage, a voltage applied between a pair of electrodes accelerates the particles. We perform simulations of the behavior of the assembly of charged particles. A normal distribution is used for the initial velocities of the assembly, with a given standard deviation. The resulting velocity distribution and its dependence on the applied voltage are analyzed. Further, the set of particles, whose pitch angles follow a normal distribution with a given standard deviation, enters a magnetic bottle where it is collimated to reduce its dispersion upon the exit of the thruster. In this second stage, we study the conditions for which the collimation produced, by the magnetic bottle, leads to the least thrust reduction. For the simulations, we assume electrons; However, the concepts apply to any charged particle species. The simulations show that the standard deviation of the pitch angle distribution has an important influence on the confinement of charged particles and on the thrust that can be generated when collimating the particle beam in a magnetic bottle.

Keywords: Collimation, Magnetic Mirror, Montecarlo, Plasma, Thrusters.

I. INTRODUCTION

The acceleration of charged particles and their behavior are of interest in several areas of science. For example, particles are naturally accelerated in Earth's atmosphere and many celestial objects. In these processes, plasma and magnetic fields are important in generating collimated beams. In solar flare events, high-velocity rays accelerate and part of the initial population precipitates to lower altitudes in the solar atmosphere. Furthermore, part of these sets heads upward and sometimes, reaches the Earth, where the charged particles are also irradiated and part of them precipitates at low altitudes in the Earth's atmosphere.

These phenomena are interesting in their own right because the charged particles that precipitate can damage and cause breakdowns in satellites and power grids. Additionally, accelerated plasma beams are widely used in today's technology and industry, such as plasma cutting and welding machines. On the other hand, the performance of cyclotrons and other particle accelerators depends on the relationship between the mass of the particles and magnetic fields. In addition, plasma beams are used in space technology, such as thrusters.

Plasma is widely used as fuel for electric thrusters because charged particles can be accelerated to high speeds, with electromagnetic fields that are relatively accessible with current technology. Electric thrusters are a system capable of accelerating a fuel by converting electrical potential energy into kinetic energy, generally electrostatic, electrothermal, electromagnetic, or a combination. They typically use inert gases as fuel, for example, krypton or argon, although xenon is more common. The main reason for using xenon is that it can generate more thrust because it has more mass.

One of the aspects to consider when using thrusters, in the case of nanosatellites, is that the resulting particle beam can impact the solar panels and the antenna. In addition to possible damage to other satellite systems, a real problem with electric thrusters is that particles hit their internal and external walls causing erosion and restricting their useful life.

In this article, we present some basic concepts related to electric thrusters. Two stages are considered, one for acceleration and another for collimation. We analyze a form of collimation using a magnetic gradient to direct the flow of particles in a way that avoids the interaction between the plasma beam and the internal walls. Collimation is a way to prevent damage from the impact of the flow on external satellite components such as solar panels and antennas. Therefore, one of the objectives of this study is to know the conditions under which the set of particles can be directed. Additionally, we estimate the percentage of thrust loss resulting from array collimation. This is done to analyze the feasibility of using magnetic mirrors as a collimation method in an electric thruster.

For this we use Monte Carlo simulations and a simplified model for the pitch angle, in which we neglect any interaction between particles, density gradients, and/or temperature changes, in addition, the angles are taken from a Gaussian distribution with deviation standard σ , this to facilitate the calculations shown.

Manuscript received on 20 June 2024 | Revised Manuscript received on 03 July 2024 | Manuscript Accepted on 15 August 2024 | Manuscript published on 30 August 2024.

Luis A. Fernández-R., Department of Space Sciences and Technology, Instituto Nacional de Astrofísica, Óptica y Electrónica, Santa María Tonantzintla, México. Email: lfernandez@inaoep.mx, ORCID ID: [0000-0003-1464-7772](https://orcid.org/0000-0003-1464-7772)

José E. Mendoza-T.*, Department of Astrophysics, Instituto Nacional de Astrofísica, Óptica y Electrónica, Santa María Tonantzintla, México. Email: mend@inaoep.mx, ORCID ID: [0000-0003-3679-3658](https://orcid.org/0000-0003-3679-3658)

© The Authors. Published by Blue Eyes Intelligence Engineering and Sciences Publication (BEIESP). This is an open access article under the CC-BY-NC-ND license <http://creativecommons.org/licenses/by-nc-nd/4.0/>

II. CHARGED PARTICLE IN A MAGNETIC MIRROR

One way to collimate an assembly of charged particles is by using a magnetic field (B) with a gradient along the field lines. In that case, we can suppose that the magnetic gradient varies as $\nabla B \parallel B$ and denote the minimum value as B_0 and the maximum value as B_m . This maximum value occurs when the density of the magnetic field lines is closer and forms a “neck”. This magnetic field structure is commonly known as a magnetic bottle, due to the shape of the field lines. If an applied electric field, collisions of any kind, or, density gradients are not considered, a charged particle leaving the region of B_0 and heading toward an area where the magnetic field is maximum, B_m , will describe a helical trajectory characterized by the gyroradius or Larmor radius r_L which depends of magnetic field intensity B and the particle’s velocity, perpendicular to the magnetic field. A detailed description of this situation can be obtained at [1], [2] and [3] [9].

$$r_L = \frac{mv_\theta}{qB} \quad (1)$$

where m and q are the mass and charge of the particle, respectively, and v_θ is the particle’s velocity perpendicular to the axis of the magnetic bottle, i.e., $v_\theta = v \sin \theta$, where θ is the angle between velocity and the axis of the bottle, called pitch angle. From (1) it can be seen that the Larmor radius will decrease as the particle heads towards a region where the intensity of the magnetic field increases. Fig. 1 shows the values of the Larmor radius for different gases commonly used as fuel in electric thrusters. We have supposed the same velocity for each gas.

The Larmor radius is an important parameter in the collimation process because it is directly related to the area covered by the particle beam. Furthermore, it allows us to know the axial component of the magnetic force that these particles will experience along their trajectory, which, in cylindrical coordinates, is expressed as

$$F_z = qv_\theta \frac{r}{2} \frac{\partial B_z}{\partial z} = \frac{mv_\theta^2}{2B_z} \frac{\partial B_z}{\partial z} \quad (2)$$

where the term $mv_\theta^2/2$ represents the kinetic energy of the particle, and the term $mv_\theta^2/2B_z$ is the kinetic energy divided by the magnetic field intensity, in other words, kinetic energy at the bottle axis. On the other hand, the potential energy U is

$$U = -\mu \cdot \mathbf{B} \quad (3)$$

where μ is the magnetic moment. This implies that the potential energy will be lower when the magnetic moment aligns with the magnetic field. The dipole moment is defined as

$$\mu = \frac{1}{2} \frac{mv_\theta^2}{B_z} \quad (4)$$

where $v_\theta = v$ and, θ is the angle formed between the velocity vector and the axis of the bottle, known as the pitch angle. Since momentum is conserved, (4) is valid for any point in the particle's trajectory.

If we divide (4) by the kinetic energy, which is also conserved, we conclude that the ratio $\sin \theta/B_z$ must also be a constant, therefore, it holds that

$$\frac{\sin^2 \theta_m}{B_m} = \frac{\sin^2 \theta_0}{B_0} \quad (5)$$

θ_0 is the pitch angle at minimum magnetic field intensity, while θ_m is the pitch angle at the location of maximum magnetic field intensity. The critical condition for the particle to reflect at the position of B_m is

$$\theta > 90^\circ \quad (6)$$

If the angle in that position satisfies

$$\theta < 90^\circ \quad (7)$$

The particle will pass through the neck of the magnetic bottle. The angle of 90° determines whether the particle reflects or passes through the bottleneck. Therefore, in (5), we can substitute the angle value $\theta = 90$ for the position of B_m and consider that, in this case, the corresponding angle at B_0 , later called θ_c , is the critical angle that makes for the particle to reflect. Then, the following equality results

$$\frac{\sin^2 90^\circ}{B_m} = \frac{\sin^2 \theta_c}{B_0} \quad (8)$$

where θ_c refers to the critical angle (in the region of the minimum magnetic field); for smaller values a particle will pass through the bottleneck. It is important to say that for θ_c and larger pitch angles, a particle will be reflected before reaching the region of the maximum magnetic field. Substituting the value of 90° (the condition to be reflected), the critical angle condition requires that the pitch angle in the minimum magnetic field (θ_0) be expressed based on a relationship between the minimum and maximum magnetic field.

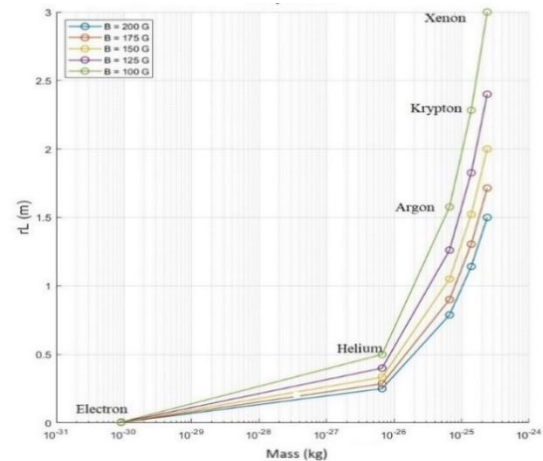


Fig. 1. Larmor radius as a function of mass. The mass of some particles, such as Xenon or Argon, is one of the main reasons for using them as fuel in Hall thrusters since their r_L is much larger than the typical size of the propellant.

$$\frac{B_0}{B_m} = \sin^2 \theta_c \quad (9)$$

This expression was obtained when we replaced B with B_m and θ for 90 degrees. Remember that if a particle has an initial angle θ_c (in the area of minimum B) it will have a larger angle as it passes through regions with larger magnetic fields.

We remember that if the particle has an initial pitch angle less than θ_c , the particle will pass through the neck of the magnetic bottle. Otherwise, the particle will be reflected by the magnetic neck. That is the reason why that area is called a magnetic mirror.

A consequence of this magnetic field structure is the decrease in the area initially covered by the electron beam as it moves towards regions of higher intensity. The relationship between these areas can be calculated from the definition of the magnetic dipole moment and its relationship with the magnetic field expressed in (4). The magnetic dipole moment of current I flowing through area A is

$$\mu = IA \quad (10)$$

In this case, I is the current generated due to the helical trajectory of the charged particle around the magnetic field lines and A is the area determined by the Larmor radius. Then, the area after collimation is obtained by equating (4) with (10).

$$A = \frac{1}{2} \frac{mv_{\perp}^2}{IB} \quad (11)$$

Using (11) we can express the magnetic field at a given position as a function of the area covered by the field lines. From this expression, we can calculate the quotient of the areas for the maximum and minimum values of B , which turns out to be

$$\frac{B_0}{B_m} = \frac{A_m}{A_0} \quad (12)$$

where A_0 and A_m correspond to the areas in the regions with the lowest and highest magnetic field intensity, respectively. It can be seen that the area ratio is inversely proportional to the magnetic field ratio. The area A_m corresponds to the neck of the magnetic bottle. If initially the particles cover a large area A_0 , in the region of B_0 , they can be concentrated in a small region as A_m , as B_m is large concerning B_0 . Thus, in a magnetic bottle, the ratio B_0/B_m determines the degree of collimation achieved for an assembly of charged particles.

III. ACCELERATION OF PARTICLES IN A UNIFORM ELECTRIC FIELD

We consider the simplest case for an assembly of electrons, a motion with constant acceleration. The movement of the particles is due to a uniform and stationary electric field, parallel to the axis of the bottle. Effects produced by collisions, forces generated by the magnetic field, or pressure gradient are not considered. Finally, we believe that the electrons follow a Maxwellian distribution function.

To create the distribution of initial velocities, from now on, initial distribution, we use a function that generates random numbers with a Gaussian distribution, centered on a given value x_c and with a standard deviation σ_x .

The initial velocity distribution has a central velocity equal to the thermal velocity v_{th} and a standard deviation σ_v (which we select according to the initial velocity dispersion we wish to analyze). From the quotient between the standard deviation of the distribution we want to generate and the standard deviation of the random distribution generated by the program, the value of a constant is calculated, defined as

$K_v = \frac{\sigma_v}{\sigma_x}$. The value of K_v is used to transform the values randomly generated by the program, to velocity values of our distribution, as follows: first, we add the thermal velocity v_{th} , which we select as the mean value, to the random numbers and multiply the values resulting by the value K_v . The thermal rate, for a given temperature T (in Kelvin), was calculated using the following equation

$$v_{th} = \sqrt{\frac{2kT}{m}} \quad (13)$$

where m is the mass of the particle and k is Boltzmann's constant. Then, we take an electron from the initial distribution and apply a voltage V_{apl} to it to accelerate it, therefore, the electric force that the electron will experience is given by

$$F_e = eV_{apl}d_{accel} \quad (14)$$

Where e is the electron charge, d_{accel} is the distance between the electrodes, that is the same over which each electron of the initial distribution is accelerated, and using a constant electric field, we calculate the acceleration experienced by each electron from the initial velocity distribution.

For the initial distribution, we use a sample of 5000 electrons with a temperature $T = 10000$ °C and an interelectrode distance $d_{accel} = 10$ cm. Furthermore, we take different values for the applied voltage, to study the behavior of the final distribution of velocities obtained for various voltages. In Fig. 2, we show histograms of the initial and final distributions, for 100, 300, 600, and 800 volts, respectively. In these cases, it can be observed that the distribution of electrons accelerated by the applied voltage V_{apl} is more asymmetric as the voltage value increases.

We also calculated the final velocities distribution of electrons for the mean temperatures of 10 °C, 100 °C, 1000 °C, and 10000 °C (Fig. 3). In each case, the applied voltage was 100 volts and the d_{accel} distance was 10 cm. We can see that the higher the temperature, the maximum of the histogram appears at higher speeds.

In the distributions plotted in Fig. 2 and Fig. 3, the direction of the initial velocity of the electrons is considered parallel to the direction of the applied electric field E . In the plots of Fig. 4, we assume that the velocity vector of the electrons makes an angle $\theta \neq 0$ degrees concerning the direction of the constant electric field, from now on called the pitch angle

We generate another set of random data to sample the electron pitch angle distribution, calculating the standard deviation of the random values generated by the program and the ratio of the desired standard deviation of the pitch angles to the standard deviation of the random values. We will refer to this relationship as K_{θ} . Finally, we multiply the initial random distribution by the constant K_{θ} .

To calculate the velocities of the electrons parallel to the electric field, we multiply the final velocity distribution by the cosine of the pitch angle distribution, before entering the magnetic field.

Thrust Generation Through a Collimated Electron Beam in a Magnetic Mirror and its Possible Applications in Plasma Thrusters

In Fig. 4, we plot three different cases for the standard deviation of the pitch angle, $\sigma_1 = 30, \sigma_2 = 60,$ and $\sigma_3 = 90$ degrees. The initial conditions of the simulations were $T = 10000$ °C, an applied voltage $V_{apl} = 100$ volts, and an acceleration distance $d_{accel} = 10$ cm. As shown in Fig. 4, as the electrons accelerate in the electric field, the slope on the high-velocity side approaches a power law.

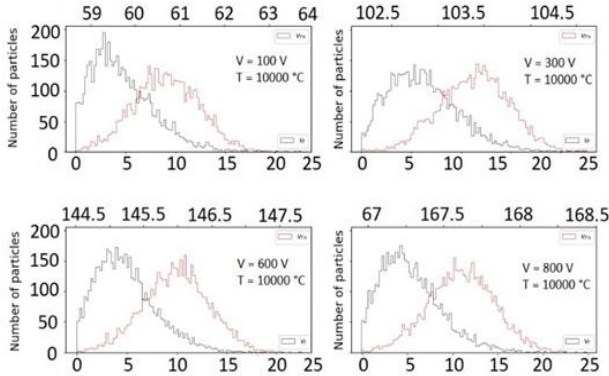


Fig. 2. Initial (red) and final (black) velocity distributions of the electrons for the same temperature and different voltages (100 V, 300 V, 600 V, 800 V). The lower axis corresponds to the initial velocity distribution and the upper axis to the final velocity distribution, multiplied by a factor of 10^7 cm/s.

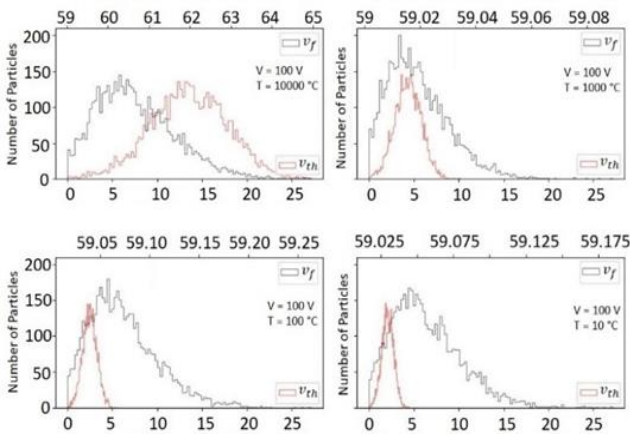


Fig. 3. Initial (red) and final (black) velocity distributions for the same voltage and different temperatures (10000 °C, 1000 °C, 100 °C, 10 °C). The lower axis corresponds to the initial velocity distribution and the upper axis to the final velocity distribution, multiplied by a factor of 10^7 cm/s.

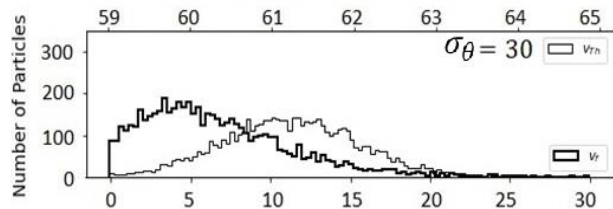


Fig. 4. Initial (soft line) and final (thick line) velocity distributions of the electrons when the velocity vector was not parallel to the electric field. The value of σ_θ represents the standard deviation considered for the pitch angle distribution. The lower axis corresponds to the initial velocity distribution and the upper axis to the final velocity distribution, multiplied by a factor of 10^7 cm/s.

IV. PARTICLE CONFINEMENT IN A MAGNETIC BOTTLE

Once the electron beam leaves the acceleration zone, it is introduced into a magnetic field to collimate it. As described in section II, the loss or reflection of a particle in a magnetic bottle depends only on its pitch angle in the region of the weakest magnetic field. Suppose we assume that the value of the angle at the end of the acceleration zone, due to the electric field, coincides with the angle that the particle has at the location of minimum magnetic field intensity B_0 , we can know if it will pass through the neck of the magnetic bottle or if it will be reflected. Recall that, if the value of the pitch angle at the position of B_0 , called θ_0 , for a charged particle, is greater than the $\sin^{-1}(B_0/B_m)^{1/2}$, then the particle is reflected. To study the confinement of electrons, we analyze the influence that the standard deviation of the pitch angle distribution (σ_θ) has on the reflection inside the magnetic mirror. A more detailed idea of the influence of σ_θ on the electron confinement can be obtained in [3] [5] [6] [7] [8]. This article only presents the case when $\sigma_\theta = 30$. Two superimposed distributions, the total number of particles in the initial distribution (soft line) and the number of reflected particles (thick line), are shown in Fig. 5, for four different cases of the magnetic field relationship in (9). In each case, the magnitude of the minimum magnetic field B_0 is the same. However, the magnitude of the maximum magnetic field, B_m , differed. We analyzed four B_m values: 25 nT, 50 nT, 75 nT, and 100 nT. It can be seen that, for small values of the magnetic field ratio ($B_0/B_m \leq 0,1$), the number of reflected particles is $\approx 53\%$.

It should be noted that complete confinement of electrons is impossible, even for minimal magnetic field ratios as seen in Fig. 6, where the field ratio is 0.001.

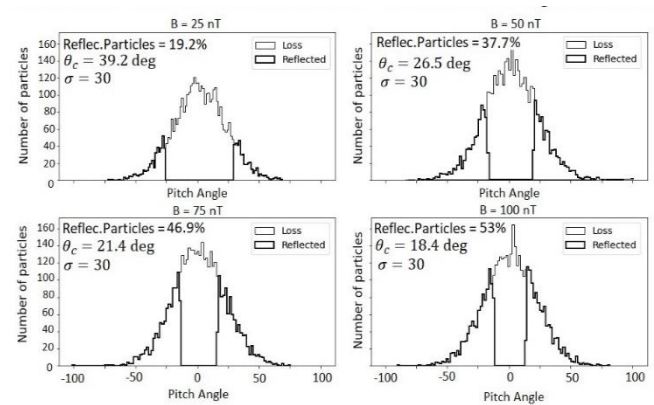


Fig. 5. Initial (dashed line) and final (continuous line) pitch angle distributions of electrons moving inside a magnetic bottle. Each plot considers different values for the maximum magnetic field B_m (25 nT, 50 nT, 75 nT, and 100 nT). θ_c represents the critical angle in equation (8). Also, the percent of reflected particles is given inside the panel for each case.

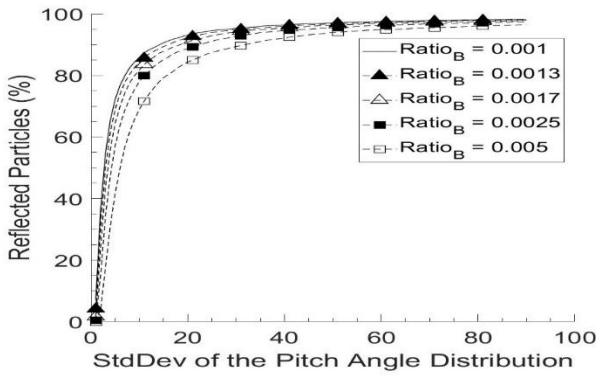


Fig. 6. Particle reflection for different magnetic field ratios. It can be seen that the percentage of reflected particles cannot reach 100%, i.e., there is no total confinement of the electron beam. The lower axis corresponds to the standard deviation of the initial pitch angle distribution.

V. THRUST

In the case of a plasma thruster, the material ejected to generate thrust corresponds to electrically charged particles that are accelerated by applying an electric field between a pair of electrodes. [4].

$$T = \frac{d}{dt}(mv_{ex}) = \dot{m}v_{ex} \quad (15)$$

where T is the thrust, m is the mass of the fuel in the spacecraft, \dot{m} is the mass flux, and v_{ex} is the exit velocity of the fuel in the spacecraft reference frame. The theory can be tested with any charged particle or ionic species. However, for the case study presented here, we will continue the analysis with the flow of electrons, but the equations remain valid for any species. We define

$$\dot{m} = MQ \quad (16)$$

where Q represents the flow rate, measured in (particles/s), and M is the atomic mass of the species [4]. In practice, it is simpler to calculate thrust using the particle beam current, I_b

$$T = \dot{m}v_{ex} = MQv_{ex} = \frac{I_b M v_{ex}}{e} \quad (17)$$

We calculate the thrust for two cases using the same number of electrons as in section III, to know its variation in each process stage: 1. After being accelerated and 2. After leaving the magnetic bottle. The initial conditions were $T = 10000$ °C, $V_{apl} = 100$ Volts, $d_{acel} = 10$ cm y $B_0 = 10$ nT. In the first case, we were interested in knowing the thrust the electrons could generate, before being accelerated, to see the amount of momentum gained after applying a voltage.

To calculate the electron current, we take the average velocity of the initial distribution and multiply it by the elemental charge, the number of particles, and the area of the thruster. Next, we use (17) to calculate the thrust. We perform this procedure for different values of the thruster area. The thrust generated by the electrons before being accelerated is shown in Fig. 7.

For the second case, we can use the fact that the motion of the particle inside the magnetic bottle is governed by the adiabatic invariance of the magnetic moment and the conservation of energy to write the following expression

$$\frac{d}{dt} \left(\frac{1}{2} m v_{\parallel}^2 + \frac{1}{2} m v_{\perp}^2 \right) = \frac{d}{dt} \left(\frac{1}{2} m v_{\parallel}^2 + \mu B \right) \quad (18)$$

where v_{\parallel} and v_{\perp} are the velocity components of the electrons, parallel and perpendicular to the axis of the magnetic bottle, respectively.

In the weak field region, B_0 , we calculate the magnetic moment, using equation (18) substituting the velocity perpendicular to the magnetic bottle, and the kinetic energy of the particles using the velocity parallel to the magnetic bottle (before and after being accelerated by the electric field).

Since the magnetic moment is invariant, we calculate the velocity perpendicular to the region where the field is strongest. Then, using energy conservation, we calculate the velocity parallel to the field at the exit of the thruster.

To know the current produced by the number of electrons leaving the magnetic bottle, we calculated the number of reflected electrons, because the sum of the particles reflected and particles leaving the magnetic bottle is the total number of electrons simulated. Using (9) and the distribution of the initial pitch angles, we can know the percentage of particles trapped in the bottle. Then, we estimate the current produced by the number of escaped electrons, and using (17) we obtain the thrust generated by these particles.

We calculate the thrust for eight values of the maximum magnetic field, $B_{m1} = 12$ nT, $B_{m2} = 14$ nT, $B_{m3} = 16$ nT, $B_{m4} = 18$ nT, $B_{m5} = 25$ nT, $B_{m6} = 50$ nT, $B_{m7} = 75$ nT y $B_{m8} = 100$ nT. We separate the eight cases into two scenarios plotted in Fig. 8 and Fig. 9, respectively. In scenario 1, in which we calculated the thrust for the first four values of the maximum magnetic field ($B_{m1} - B_{m4}$), we found that the thrust reduction was approximately 25% of its maximum value (i.e., the thrust generated by the electrons just after being accelerated by the electric field). In the second scenario (where we consider the magnetic field values $B_{m5} - B_{m8}$), the reduction was approximately 60%. In both scenarios, the greater the standard deviation of the firing angle, for a given value of the magnetic field ratio, the greater the number of confined electrons.

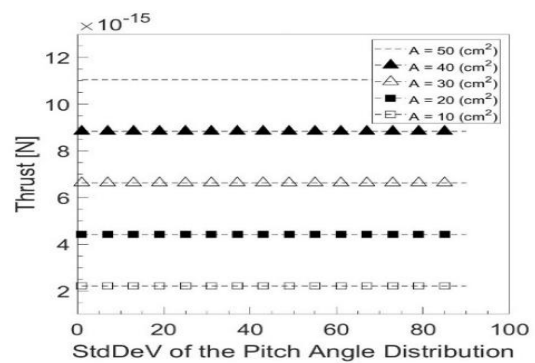


Fig. 7. Values corresponding to Case 1. The thrust generated by the electron beam after being accelerated is for the first case studied in section III, where the velocity vector and the electric field are parallel. The parameter A corresponds to the area the electrons cover after being collimated.

Thrust Generation Through a Collimated Electron Beam in a Magnetic Mirror and its Possible Applications in Plasma Thrusters

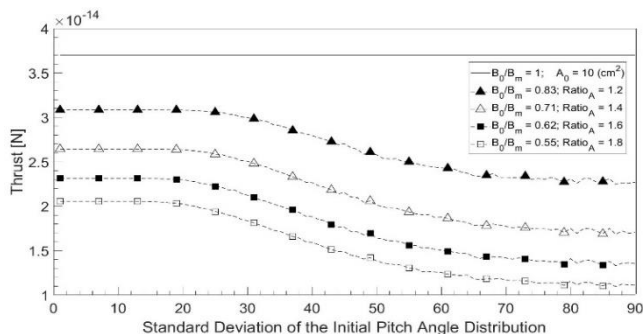


Fig. 8. Values corresponding to Case 2. Thrust generated by the electron beam after being accelerated, for the first four magnetic field relations. This case corresponds to the second case studied in section III. The parameter A corresponds to the area the electrons cover after being collimated.

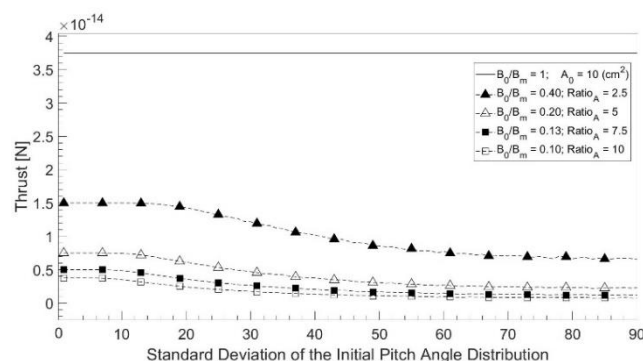


Fig. 9. Values corresponding to Case 2. Thrust generated by the electron beam after being accelerated, for the second four magnetic field relations. This case corresponds to the second case studied in section III. The parameter A corresponds to the area the electrons cover after being collimated.

Finally, Table 1 shows the thrust values for the different magnetic field ratios, Fig. 8 and Fig. 9, and the standard deviation analyzed in section IV ($\sigma_\theta = 30$).

Table 1. Thrust as a Function of the Ratio of Magnetic fields to $\sigma_\theta = 30$.

Ratio B_0/B_m	Critical Angle	Trapped Particles (%)	Thrust (N) ($\sigma_\theta = 30$)
1.00	90	0	3.74e-14
0.83	56.1	2.5	2.94e-14
0.71	45.2	4.8	2.46e-14
0.62	38.3	7.1	2.09e-14
0.55	33.4	9.7	1.81e-14
0.40	23.6	16.7	1.21e-14
0.20	11.5	36.4	4.64e-15
0.13	7.5	46.3	2.59e-15
0.10	5.7	52.5	1.69e-15

VI. DISCUSSION

As shown in Fig. 6, the curves of the number of reflected particles show two different behaviors, in two ranges of values of the standard deviation distribution of the initial pitch angle σ_θ . In the 0 to 20 degrees range, the percentage of reflected particles increases rapidly with σ_θ . Conversely, in the 20 to 90 degree range, the percentage of reflected particles increases slowly with σ_θ . Furthermore, in the same figure it can be seen that the value of σ_θ seems to have more influence than the ratio B_0/B_m for values of $\sigma_\theta \geq 10$ degrees, for example, for a ratio of magnetic fields equal to 0.001, the following percentages are obtained of reflected particles with

the standard deviations $\sigma_\theta = 30, 60$ and 90 : 93%, 97,8% y 98,56%, respectively. This fact shows that, for ratios $B_0/B_m \leq 0.005$, the electron pitch angle does not have much relevance in the percentage of trapped particles, as long as $\sigma_\theta > 20$. This fact can also be observed in figures 8 and 9, where the thrust is strongly reduced for standard deviations $\sigma_\theta > 20$. Suppose the purpose of the bottle is to retain a large number of electrons, the option to avoid large magnetic fields is to increase the standard deviation of the pitch angle distribution; this allows increasing the percentage of particles whose angle is greater than the critical angle.

VII. CONCLUSION

The percentage of reflected particles, for $B_0/B_m < 0,01$, is large for pitch angle distributions with standard deviations $\sigma_\theta > 10$ degrees. That is, the standard deviation does not have much relevance to prevent particles from reflecting. On the other hand, for $B_0/B_m > 0,1$ the standard deviation plays an important role in preventing the particles from reflecting.

The simulations allow us to see how critical the initial angle is in causing the reflection of large numbers of particles.

We find that up to a ratio $B_0/B_m < 0,66$, not much thrust is lost for standard deviations $\sigma \leq 30$ of the pitch angle distribution.

DECLARATION STATEMENT

Funding	Yes, I have received financial support for this article. This work was supported by the National Council of Humanity, Science and Technology through grant number: 906469.
Conflicts of Interest	No conflicts of interest to the best of our knowledge.
Ethical Approval and Consent to Participate	No, the article does not require ethical approval and consent to participate with evidence.
Availability of Data and Material	Not relevant.
Authors Contributions	All authors have equal participation in this article.

REFERENCES

- CHEN, FRANCIS F., "Introduction to plasma physics and controlled fusion", 3a ed, Springer, (2016). <https://doi.org/10.1007/978-3-319-22309-4>
- GOLDSTON, R.J., RUTHERFORD, P. H., "Introduction to plasma physics", IOP. Bristol, UK (1995). <https://doi.org/10.1201/9781439822074>
- FERNANDEZ-RAMOS L.A., MENDOZA-TORRES J.E., GOMEZ-FLORES O., TIRADO-BUENO E., "Charged Particle Reflection in a Magnetic Mirror", Accepted for publication in: Revista Mexicana de Física E., 2023. <https://doi.org/10.31349/RevMexFisE.21.020211>
- DAN M. GOEBEL, IRA KATZ, "Fundamentals of Electric Propulsion: Ion and Hall Thruster", Jhon Wiley and Sons, Hoboken, New Jersey, (2008). <https://doi.org/10.1002/9780470436448>
- Asari, A. R., Guo, Y., & Zhu, J. (2020). Magnetic Properties of Somaloy 700 (SP) Material Under Round Magnetic Flux Loci. In International Journal of Innovative Technology and Exploring Engineering (Vol. 9, Issue 3, pp. 2479–2483). <https://doi.org/10.35940/ijitee.c9226.019320>
- N, K. K., Kiran, D. K. S., Ragav, L. Y., & Kiran B, M. (2020). An Innovative Device to Monitor Material Quality using Magnetic Permeability. In International Journal of Recent Technology and

- Engineering (IJRTE) (Vol. 8, Issue 6, pp. 3128–3133).
<https://doi.org/10.35940/ijrte.f8747.038620>
7. Kumar, C., Sinha, A. R., Prakash, S., Singh, K., & Kumar, S. (2020). Water Purification by Activation Plasma Technology. In International Journal of Innovative Science and Modern Engineering (Vol. 6, Issue 8, pp. 15–23). <https://doi.org/10.35940/ijisme.h1251.076820>
 8. Gupta, Mr. R., Singhal, Dr. T., & Verma, Dr. D. (2019). Quantum Mechanical Reflection and Transmission Coefficients for a Particle through a One-Dimensional Vertical Step Potential. In International Journal of Innovative Technology and Exploring Engineering (Vol. 8, Issue 11, pp. 2882–2886). <https://doi.org/10.35940/ijitee.k2424.0981119>
 9. Tyagi, R. K., Joshi, P., & Pandey, R. S. (2022). Investigation of Various Parameters in Magneto-Rheological Dampers. In International Journal of Engineering and Advanced Technology (Vol. 11, Issue 3, pp. 135–140). <https://doi.org/10.35940/ijeat.c3371.0211322>

AUTHORS PROFILE



Luis Ángel Fernández Ramos. He was born in Orizaba city, Mexico, where he obtained a Bachelor's degree in mechanical engineering in 2015 at the Tecnológico Nacional de México and a Master's degree in Space Science and Technology (CyTe) at the Instituto Nacional de Astrofísica, Óptica y Electrónica (INAOE) in 2021. He

is currently a second-year PhD student at the INAOE, developing research on instabilities in magnetized, weakly ionized plasmas, for applications in space propulsion. He has 3 publications and some participation in national and international conferences. His interest includes Plasma Physics, Fluid Mechanics, and Electric Propulsion.



José Eduardo Mendoza Torres. He was born in Puebla city, Mexico, where he studied until his Bachelor's degree in Physics, at the Faculty of Physics and Mathematics of the Universidad Autónoma de Puebla. He worked for a year at this faculty, teaching Physics courses. He received his Ph.D. at the Special Astrophysical Observatory, in

Saint Petersburg, Russia. After that, he joined the Astrophysics department of Instituto Nacional de Astrofísica, Óptica y Electrónica, where he has taught, researched, and supervised thesis since then. His interest includes solar activity, galactic masers, and space technology. He has published more than 60 scientific papers. Also, he has been in charge of the National Olympiad of Astronomy in Mexico since 2002 until now.

Disclaimer/Publisher's Note: The statements, opinions and data contained in all publications are solely those of the individual author(s) and contributor(s) and not of the Blue Eyes Intelligence Engineering and Sciences Publication (BEIESP)/ journal and/or the editor(s). The Blue Eyes Intelligence Engineering and Sciences Publication (BEIESP) and/or the editor(s) disclaim responsibility for any injury to people or property resulting from any ideas, methods, instructions or products referred to in the content.